J. Astrophys. Astr. (2006) **27,** 255–265

Photospheric, Chromospheric and Helioseismic Signatures of a Large Flare in Super-active Region NOAA 10486

Ashok Ambastha
Udaipur Solar Observatory, Physical Research Laboratory, Udaipur 313 001, India.
e-mail: ambastha@prl.res.in

Abstract. NOAA 10486 produced several powerful flares, including the 4B/X17.2 superflare of October 28, 2003/11:10 UT. This flare was extensively covered by the H_α and GONG instruments operated at the Udaipur Solar Observatory (USO). The central location of the active region on October 28, 2003 was well-suited for the ring diagram analysis to obtain the 3-D power spectra and search for helioseismic response of this large flare on the amplitude, frequency and width of the p-modes. Further, using USO observations, we have identified the sites of new flux emergences, large proper motions and line-of-sight velocity flows in the active region and their relationship with the flare.

Key words. Solar flares—flare trigger—ring diagram.

1. Introduction

Solar flares are usually associated with prominent chromospheric and coronal signatures, and in exceptional events even at the photospheric level. The basic flare eruption is believed to occur due to a magnetohydrodynamic (MHD) catastrophe, driving a reconnection process in the magnetic field lines stretched out by the eruption (Priest & Forbes 2002). Extensive efforts have been made to identify the conditions and magnetic topology leading to the onset of flares and CMEs, viz., sigmoid formation along quasi-separatrix layers (Fletcher *et al.* 2001; Gibson *et al.* 2002), magnetic helicity injection by photospheric motions (Zhang & Wang 2002a), rapid magnetic field changes before the onset of flare (Wang *et al.* 2002; Spirock *et al.* 2002), magnetic shearing (Ambastha *et al.* 1993), intrusion of adjacent magnetic feature (Ulrich *et al.* 2002), magnetic flux emergence (Zhang & Wang 2002b; Kurokawa *et al.* 2002), etc. Also, moderate flares may occur where newly emerged flux gets cancelled with opposite polarity, presumably by reconnection (Martin *et al.* 1984; Ambastha & Mathew 2000; Jennings *et al.* 2002), and can trigger the release of magnetic energy stored in a larger volume (Priest 1984).

During October 18–November 5, 2003, three large sunspot groups, NOAA 10484, 10486 and 10488, were observed which produced 140 flares; 11 of which were X-class. Super-active region NOAA 10486 accounted for most of these extremely energetic flares. Figure 1 shows the GOES soft X-ray flux profile for October 26–31, 2003 showing two of its major flares which occurred when NOAA 10486 was located close to the solar disk-center. The record-setting flare of November 4, 2003 occurred when

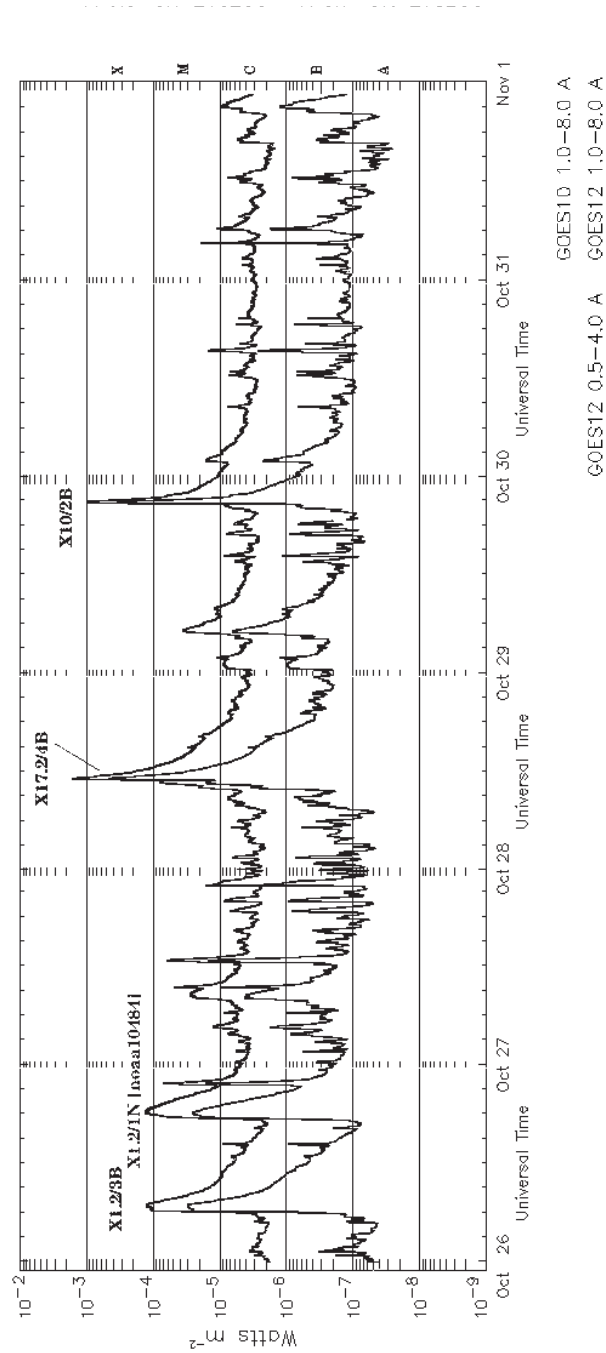

Figure 1. GOES disk-integrated soft X-ray flux showing the two major flares, X17.2 and X10, of NOAA 10486 which occurred during October 26–31, 2003.

NOAA 10486 reached the west-limb. This flare of unprecedented magnitude which saturated the GOES X-ray detectors was first classified as X28/3B flare, but later re-classified as an X45 $\pm$ 5 flare based on its ionospheric response (Thomson *et al.* 2004). Most of these energetic flares were associated with fast moving CMEs, which continued to occur even as the active region rotated off the west-limb. Due to its central location on the disk, the 4B/X17.2 flare event of October 28, 2003/11:10 UT and associated proton storm and CME had much larger geomagnetic effects as compared to the larger X45 flare which occurred at the limb. The total solar irradiance (TSI) due to this flare recorded an increase by 360 mW/m^2, the first such unambiguous detection since the beginning of routine TSI measurements in 1978 (Woods *et al.* 2004). We have selected this flare for detailed analysis of its photospheric, chromospheric and helioseismic signatures due to the favourable location of the active region near the CMP which minimizes the projection effects.

2. The observational data

High cadence H_α filtergrams were obtained from USO providing extensive coverage of the active regions NOAA 10484, 10486 and 10488 during the period of October 18–November 5, 2003. In addition, magnetograms and dopplergrams were also obtained at a cadence of 1-minute by the GONG+ instrument operated at USO. Using movies made from these observations, we attempt to identify the sites of magnetic flux changes, chromospheric restructuring, and the doppler velocity changes in the active region, particularly around the site of flare onset. The two other large regions, NOAA 10484 and 10488, were also observed during this period, however, they showed considerably lower flare productivity as compared to NOAA 10486.

3. Evolution of NOAA 10486 and the 4B/X17.2 flare

Figure 2 shows daily evolution of chromospheric structures of NOAA 10486 using H_α-filtergrams obtained from USO during October 26–31, 2003. A long curved filament 'a' was seen to meander through the middle of the active region on October 26, 2003 from which a smaller filament 'b' branched out. This system of filaments went through a major structural change on October 27, 2003 forming a 'channel' of opposite polarity region between them, marked as 'c'. Yang *et al.* (2004) reported strong shear flows along the magnetic neutral line, i.e., the filament 'c'. Zirin & Wang (1993) earlier discovered such magnetic 'channel' structures of elongated mixed polarity regions with strong shear flows along them. Harvey & Harvey (1976) have also found strong horizontal shear flows in flaring regions, and suggested them to be an important factor in flare production. This appears to be a common feature of all superactive regions. As seen from the filtergram of October 28, 2003, the channel gradually became narrower as a result of significant spatial changes taking place in the active region. Interestingly, this channel was the site of the onset of the 4B/X17.2 superflare of October 28, 2003 (Fig. 3). Before the 4B flare, several smaller flares occurred in the neighbouring locations. Chromospheric structural changes were observed subsequent to the superflare, for example, the filament 'd' disappeared, disconnection of 'b' occurred as marked at 'e' (Fig. 2: October 29 frame). New active filaments formed later during October 30–31, 2003 at the location 'c' indicating significant magnetic restructuring. The active

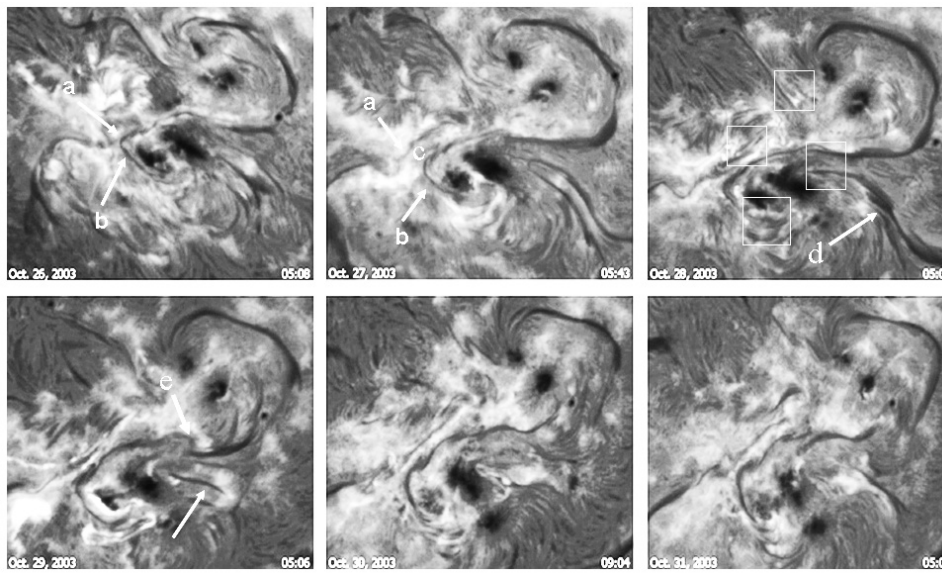

Figure 2. USO H_α filtergrams of NOAA 10486 during 26–31 October 2003 showing the evolution of chromospheric structures.

region retained its large magnetic complexity, and contained sufficient energy even after the superflare of October 28, 2003; evident from the fact that a large 2B/X10 white light flare followed at 20:37 UT on October 29, 2003. NOAA 10486 was estimated to possess an order of magnitude greater free energy than that in two other active regions NOAA 10484 and NOAA 10488 on October 29, 2003 (Metcalf *et al.* 2005).

Figure 3 shows the spatial and temporal evolution of the 4B/X17.2 super-flare in H_α. Negative filtergrams have been used for showing the structural details of the flare-ribbons more clearly. After the preflare activation seen in 10:39:28 UT frame, the flare erupted impulsively, reaching a maximum phase at 11:10:05 UT. The bright flare-ribbons separated away rapidly; a typical property of two-ribbon flares. Post-flare loops, generally observed during the decay phase, appeared as seen in the 11:14:46 UT frame, while the flare lasted over much longer. Notably, the H_α filtergrams showed formation of a twisted rope-like structure in the magnetic channel, rising upwards and eventual eruption of the filament.

4. *GONG+* magnetic and velocity field observations

Movies of $GONG+$ velocity and line-of-sight magnetic field maps obtained during October 28, 2003, showed significant evolutionary changes at several locations along the magnetic channel and in the vicinity of the elongated filament. This is as shown in Fig. 4 in which L-O-S magnetogram contours, at ± 10, ± 500, $\pm 1500\,G$ levels, are overlaid on the $GONG+$ dopplergrams. Development of an increasing downward flow was seen in box '3', where the filament was destabilized. On the other hand, enhancement of upward directed flow was observed in box '2', where a positive polarity flux emerged. In box '1', which covers location of the H_α twisted rope structure, moving blue shift events were observed. These evolved considerably during the time

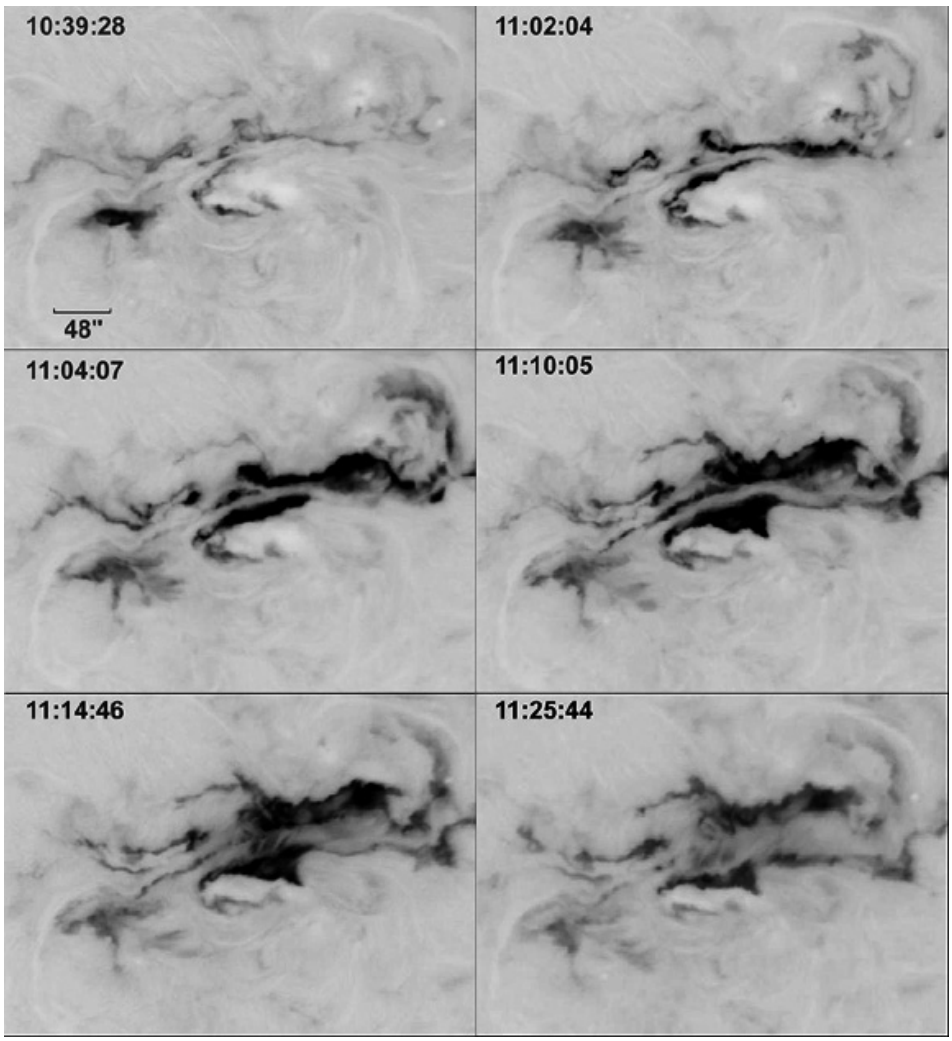

Figure 3. USO H_α filtergrams the 4B/X17.2 flare of October 28, 2003. Filtergrams are shown in 'negative'.

of the flare onset. Such events are indicators of upflow from reconnection events that are found to be 5 times more frequent before eruptive flares than in noneruptive flares (DesJardins & Canfield 2003), and upflows in the range of 40–80 km s^{-1} have been detected during the pre-flare phase (Brosius & Phillips 2004). Keil *et al.* (1994) found that flare kernels are locations of shear in vertical photospheric flows and locations of convergence in horizontal photospheric flows. Meunier & Kosovichev (2003) have also found evidence of persistent, supersonic downflows and shear flows in flaring active regions.

Several attempts have been made in the past to monitor the changes in magnetic flux, shear and electric currents before, during and after flares (Ambastha *et al.* 1993; Chen *et al.* 1994; Kosovichev & Zharkova 2001; Meunier & Kosovichev 2003; Yurchyshyn *et al.* 2004). Spirock *et al.* (2002) carried out a magnetic flux analysis for the large X20

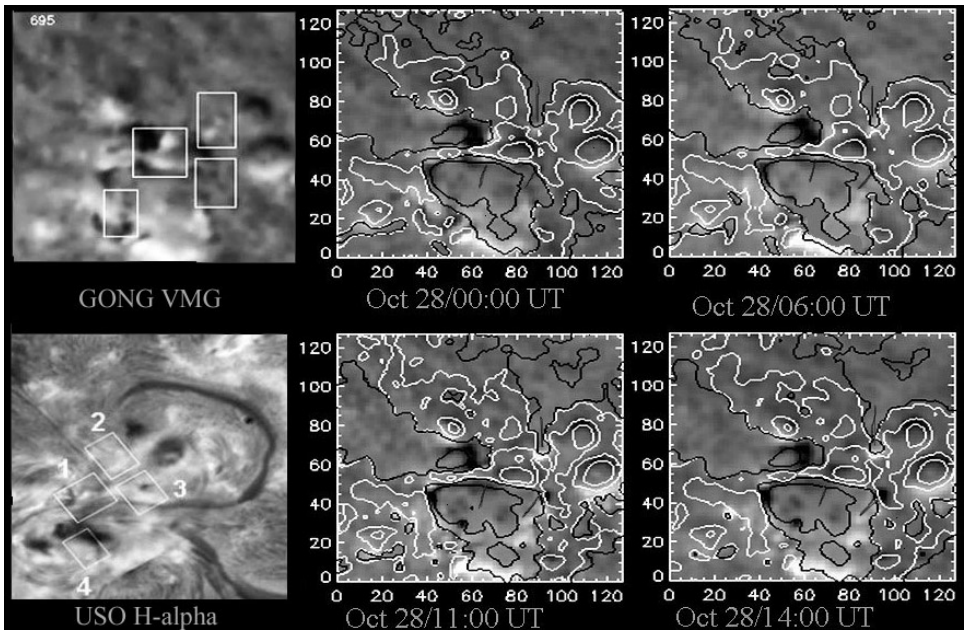

Figure 4. Overlays of GONG+ Dopplergrams (grey-level images) and line-of-sight magnetograms (contours). Selected areas-of-interest are shown over GONG VMG and USO H_α images.

flare of April 2, 2001, and reported an increase by 6×10^{20} Mx in the leading polarity, and no clear change in the following polarity. Wang *et al.* (2002) showed similar flux variation for six other X-class flares. However, the changes in the magnetic field twist parameter was statistically found insufficient to distinguish between flaring and non-flaring active regions (Leka & Barnes 2003). Recently, using GONG+ magnetograms, Sudol & Harvey (2005) have reported statistically significant changes in magnetic flux related with flares. However, it is important to consider flare-related changes in photospheric spectral lines while deriving such inferences, as this may seriously affect magnetic field calculations (Abramenko & Baranovsky 2004; Edelman *et al.* 2004).

Using the GONG+ Doppler (line-of-sight) velocity and magnetic data-cubes taken at a cadence of 1 minute, we have evaluated the net magnetic flux and Doppler velocity during 2003, October 27/12:26–October 28/16:09 UT for the four subareas marked by the boxes in Fig. 4. Time profiles for these tracked regions are given in Fig. 4. The evolutionary trend of flux variation for the boxes '1', '2' and '3' is found to go through a change before and after the time of the flare maximum marked by an arrow. Of course, the spikes at the flare maximum are probably caused by the changes of spectral line at that time. On the other hand, net flux for the box '4', located in a flare-quiet area, shows only a gradual decreasing trend of evolution. The profiles of net Doppler velocity have larger scatter, and any flare-related changes are not obvious.

These observed flux changes may occur due to a variety of processes, such as, emergence or submergence of flux and horizontal motions leading to the enhancement or cancellation of fluxes. GONG VMG movie shows such features at several locations during the course of the flare. It is known that photospheric horizontal motions of magnetic fluxes could lead to the accumulation of magnetic energy in a flare current

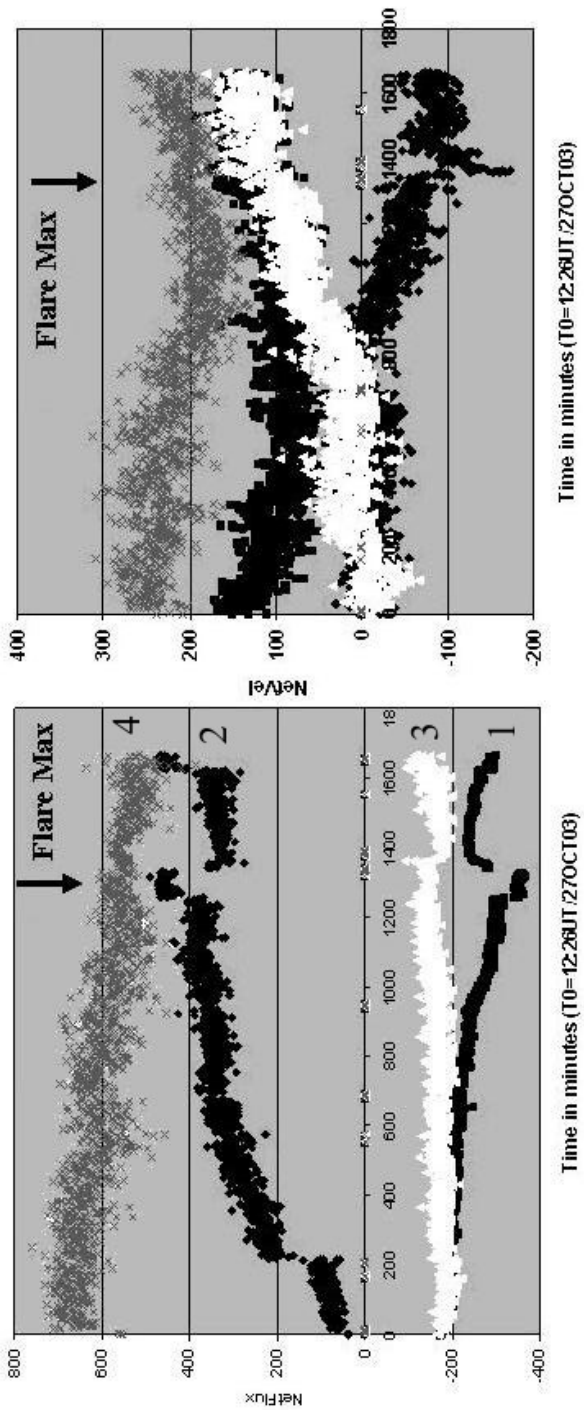

Figure 5. Temporal variations in net magnetic fluxes and Doppler velocity in the selected areas of interest.

sheet of the order of $10^{32} \sim 10^{33}$ ergs (Bilenko *et al.* 2002), and twisting of magnetic loops may result into kink instability and eventual release of 35–50% of the free magnetic energy (Gerrard *et al.* 2002). Also, magnetic modelling of flares has revealed onset of flare due to reconnection of emerging flux in a sheared magnetic field (Berlicki *et al.* 2004; Brooks *et al.* 2003). Appearance of certain horizontal velocities may lead to changes in local magnetic field structures, and generate electric current systems (Martres *et al.* 1982; Fontenla *et al.* 1995).

5. Helioseismic signatures of the flare

It is generally accepted that acoustic modes are always present on the Sun, excited by turbulence in the convection zone (Goldreich & Kumar 1988). Transient phenomena, such as flares and CMEs may contribute additional energy to these modes. However, using GONG+ time series of low-l p-mode power for the period of May 01, 1995–December 31, 2001, a mild anti-correlation is found on a global scale with disk-integrated flare-index and CME-counts (Ambastha & Antia 2004). It is interesting to ask if large flares or CMEs may have any effect on p-modes on the smaller spatial scales of active regions. Although most of the flare energy is released in the chromosphere and corona, the white light flares imply that a part of energy may be deposited in the photosphere, affecting the modes of solar oscillation as reported by Kosovichev and Zharkova (1998, 1999) and Donea *et al.* (1999). The effect of flares on solar oscillation modes has been further explored for several active regions using the ring diagram technique (c.f., Hill 1988) by obtaining 3D spectra before, during and after the flares, giving evidence of variation in mode characteristics such as frequency, width, power and asymmetry (Ambastha *et al.* 2003). At the time of 4B/X17.2 superflare, NOAA 10486 was located ideally at the disk-center and the flare was energetically substantial to look for any flare related effects on the p-mode characteristics. Figure 6 shows that frequencies and widths of the modes are not affected significantly during the three-day period around the flare, i.e., October 27–29, 2003. However, the mode-amplitude increased substantially after the large flare of October 28, 2003 (left panel). It increased further on October 29, 2003 (right panel), as a result of more flares after the superflare of October 28, 2003 (Ambastha *et al.* 2004). Recent studies have shown that subsurface flows may also lead to p-mode characteristic variations (Zhao & Kosovichev 2004; Haber *et al.* 2004).

We have used the regions tracked for 8192 minutes around the central meridian passage, and inverted the frequency differences to calculate sound speed between an active and quiet region for NOAA 10484, 10486, and 10488. This has been carried out by using the two common methods of solving the inversion integral, viz., the Regularized Least Squares (RLS) (Antia & Basu 1994), and Optimally Localized Averages (OLA) (Pijpers & Thompson 1992). These two inversion methods are complimentary in nature, therefore, one can be more confident if OLA and RLS results are in good agreement (Basu *et al.* 2004). It is found that the sound speed in active regions was lower just below the surface but at depths exceeding 7 Mm, the trend reversed. Similarly, the fitted velocities for each mode is inverted to calculate the meridional (u) and zonal (v) components as a function of depth (Ambastha *et al.* 2004). A steep gradient in meridional velocity is found to exist below a depth of 4 Mm which appears to be correlated with flares (Fig. 7) as similar a feature was also observed for other major active regions such as NOAA 9026 and 9393 (Ambastha *et al.* 2003).

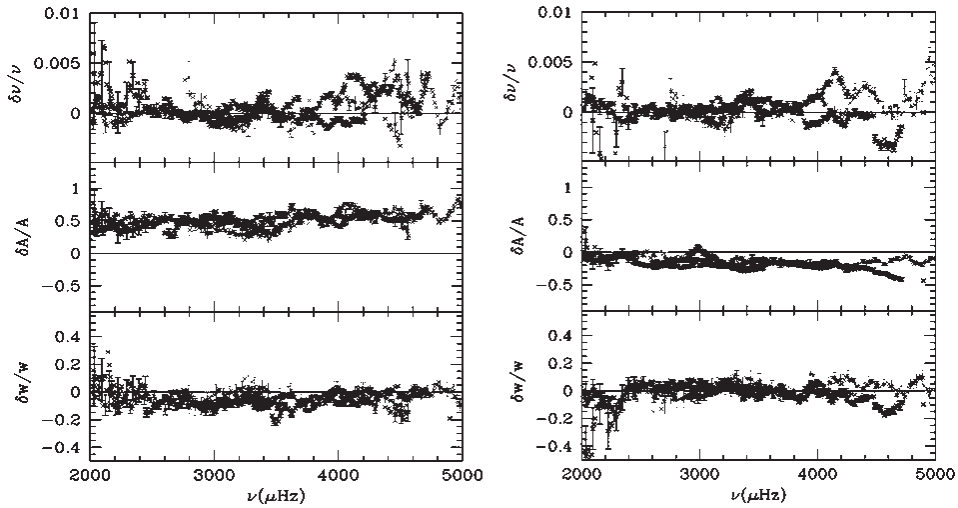

Figure 6. The relative difference in mode frequencies, widths and ratio of peak power for NOAA 10486 using ring-diagram analysis. The left and right panels respectively show the results for p-modes with $n = 0, 1, 2, 3$ obtained for the flare/pre-flare (i.e., Oct. 28/Oct. 27) and the flare/post-flare (i.e., Oct. 28/Oct. 29) phases.

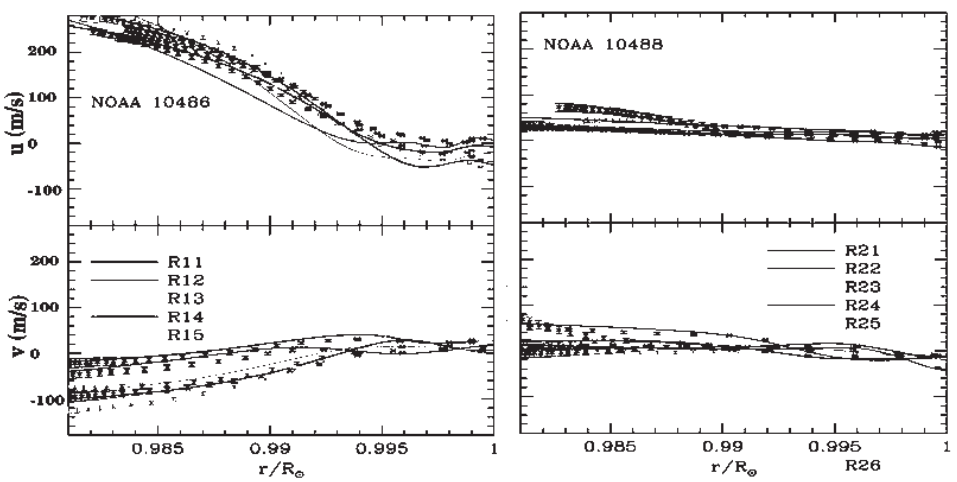

Figure 7. The meridional (u) and zonal (v) components of velocity for NOAA 10486 and 10488 at different stages. The lines show the results obtained using RLS inversions, while points mark those obtained using OLA (*c.f.*, Ambastha *et al.* 2004).

6. Conclusions

Net flux and Doppler velocity have been obtained at several locations in NOAA 10486 using GONG data during October 28–29, 2003, which show variations before and after the X17.2 flare of October 28, 2003. The Doppler maps show that upward (and downward) flows developed near the large H_α filament, associated with new

emerging fluxes. This process could have destabilized the filament delineating the narrow channel. The filament erupted along with the flare, which perhaps resulted in the fast Earth-ward moving CME. After the flare, the filament was partially restored with significant restructuring and disconnection. Evidence of reconnection was observed at the site of flux emergence prior to the flare onset. We found significant increase in the power of the accoustic modes during the X17 flare, which was beyond the normal value expected from the influence of magnetic fields. In addition, the meridional velocity in the flaring region was found to have a steep gradient below a depth of 5 Mm.

References

Abramenko, V. I., Baranovsky, E. A. 2004, *Solar Phys.*, **220**, 81.
Ambastha, Hagyard, West 1993, *Solar Phys.*, **148**, 277.
Ambastha, A., Mathew S. K. 2000, *Solar Phys.*, **197**, 75.
Ambastha, A., Basu, S., Antia, H. M. 2003, *Solar Phys.*, **218**, 151.
Ambastha, A., Antia H. M. 2004, In: Proc. SOHO 14/GONG 2004 Workshop, ESA SP-559, p. 289.
Ambastha, A., Basu, S., Antia, H., Bogart, R. 2004, Proc. SOHO 14/GONG 2004 Workshop, ESA SP-559, p. 293.
Antia, H. M., Basu, S. 1994, *Astron. Astrophys. Suppl.*, **107**, 421.
Basu, S., Antia, H. M., Bogart, R. S. 2004, *ApJ*, **610**, 1157.
Berlicki, A., Schmieder, B., Vilmer, N., Aulanier, G., Del Zanna G. *et al.* 2004, *Astron. Astrophys.*, **423**, 1119.
Bilenko, I. A., Podgorny, A. I., Podgorny, I. M. 2002, *Solar Phys.*, **207**, 323.
Brooks, D. H., Kurokawa, H., Yoshimura, K., Kozu, H., Berger, T. E. 2003, *Astron. Astrophys.*, **411**, 273.
Brosius, J. W., Phillips, K. J. H. 2004, *ApJ*, **613**, 580.
Chen, J., Wang, H., Zirin, H., Ai, G. 1994, *Solar Phys.*, **154**, 261.
DesJardins, A. C., Canfield, R. C. 2003, *ApJ*, **598**, 678.
Donea, A.-C., Braun, D. C., Lindsey, C. 1999, *ApJ*, **513**, L143.
Fletcher, L., Metcalf, T. R., Alexander, D., Brown, D. S., Ryder, L. A. 2001, *ApJ*, **554**, 441.
Edelman, F., Hill, F., Howe, R., Komm, R. 2004, In: Proc. SOHO 14/GONG 2004 Workshop, ESA SP-559, p. 416.
Fontenla, J. M., Ambastha, A., Kalman, B., Csepura, Gy. 1995, *ApJ*, **440**, 894.
Gerrard, C. L., Arber, T. D., Hood, A. W. 2002, *Astron. Astrophys.*, **387**, 687.
Gibson S. E. *et al.* 2002, *ApJ*, **574**, 1021.
Goldreich, Kumar 1988, *ApJ*, **326**, 462.
Haber D. A., Hindman B. W., Toomre J., Bogart R. S., Thomson M. J., LohCo Team 2004, *Astron. Astrophys. Suppl.*, **204**, 02.11.
Harvey, K. L., Harvey, J. W. 1976, *Solar Phys.*, **47**, 233.
Hill, F. 1988, *ApJ*, **333**, 996.
Jennings, D. E. *et al.* 2002, *ApJ*, **568**, 1043.
Keil, S. L., Balasubramaniam, K. S., Bernasconi, P., Smaldone, L. A., Cauzzi, G. 1994, *Astron. Soc. Pac. Conf. Ser.*, **68**, 265.
Kosovichev, A. G., Zharkova, V. V. 1998, *Nature*, **393**, 317.
Kosovichev, A. G., Zharkova, V. V. 1999, *Solar Phys.*, **190**, 459.
Kosovichev, A. G., Zharkova, V. V. 2001, *ApJ*, **550**, L105.
Kurokawa H., Wang T. J., Ishii, T. T. 2002, *ApJ*, **572**, 598.
Leka K. D., Barnes G. 2003 *ApJ*, **595**, 1277; 1296.
Martin, S. F. *et al.* 1984, *Adv. Space Res.*, **4**, 61.
Martres, M. J. *et al.* 1982, *PASJ*, **34**, 299.
Metcalf, T. R., Leka K. D., Mickey D. L. 2005, *Astrophys. J*, **623**, L53.
Meunier, N., Kosovichev, A. 2003, *Astron. Astrophys.*, **412**, 541.
Pijpers, F. P., Thompson, M. J. 1992, *Astron. Astrophys.*, **262**, L33.
Priest, E. R. 1984, *Adv. Space Res.*, **4**, 37.

Priest, E. R., Forbes T. G. 2002, *Astron. Astrophys. Rev.*, **10**, 313.
Spirock, T. J., Yurchyshyn, V. B., Wang, H. 2002, *ApJ*, **572**, 1072.
Sudol, J. J., Harvey, J. W. 2005, *ApJ*, **635**, 647.
Thomson, N. R., Rodger, C. J., Dowden R. L. 2004, *Geophys. Res. Lett.*, **31**, L06803.
Ulrich, R. K. *et al.* 2002, *ApJS*, **139**, 259.
Wang, H. *et al.* 2002, *ApJ*, **576**, 497.
Woods, T. N., Eparvier, F. G., Fontenla, J. *et al.* 2004, *Geophys. Res. Lett.*, **31**, L10802.
Yang, G., Xu, Y., Cao, W., Wang, H., Denker, C., Rimmele, T. R. 2004, *ApJ*, **617**, L151.
Yurchyshyn, V. B. *et al.* 2004, *ApJ*, **605**, 546.
Zhang, J., Wang, J. 2002a, *ApJ*, **566**, L117.
Zhang, C., Wang, J. 2002b, *Solar Phys.*, **205**, 303.
Zhao, J., Kosovichev A. G. 2004, *ApJ*, **603**, 776.
Zirin, H., Wang, H. 1993, *Nature*, **363**, 426.